A Strategy for Controlling the Central Torsion Angle in Biphenyl-Based Molecular-Scale Bridges

Andrew C. Benniston,*[a] Anthony Harriman,[a] Pritesh V. Patel,[a] and Craig A. Sams[a]

Keywords: Crown ether / Cation binding / Molecular dynamics simulations / Fluorescence / Molecular modelling

The synthesis of a series of crown ether ligands (**C4**–**C6**) based upon the 2,2′-biphenyl unit is described. In the series, the length of the polyether chain connecting the two oxygen atoms increases progressively. These polyethers are moderately fluorescent in acetonitrile solution, but this emission is partially quenched upon the addition of various alkali metal cations. Spectrofluorimetric titrations performed with $MClO_4$ (M = Li^+, Na^+) or KPF_6 show that binding to crown ethers **C4**–**C6** involves the formation of a 1:1 cation/ligand complex. The geometry of the resultant complex depends on the nature of the bound cation and also on ionic strength. In particular, the photophysical properties of the polyether are sensitive to the torsion angle around the central connector in the biphenyl group. This approach, therefore, could be used to systematically vary the dihedral angle for biphenyl-based molecular-scale bridges.

Introduction

One of the more important unanswered questions in the field of electron-transfer reactions concerns the effect of dihedral angle on the electronic coupling matrix element.[1] Although theoretical studies have been aimed at this issue,[2] experimental studies have been hampered by the lack of suitable model compounds. Attempts to vary the central torsion angle in biphenyl bridges, for example, have relied on the introduction of bulky groups at the *ortho* positions.[3] Whilst influencing the torsion angle, this approach also perturbs the electronic properties of the bridge. A possible alternative is to build the biphenyl bridge into a macrocyclic polyether of variable size.[4] Here, the torsion angle should be determined by the length of the polyether strap, and fine-tuning should be achieved by binding different cations in the cavity defined by the polyether. It is well known that cation binding has the effect of rigidifying the polyether,[5] but it is less clear that the torsion angle will be affected. We now examine if this is a viable strategy for the construction of multicomponent photonic devices having biphenyl-based bridges of precisely defined geometry.

Since the serendipitous discovery of crown ethers by Pedersen[6] in the 1960s, their applications in the field of chemistry have been widespread. Typical examples of their use include phase-transfer catalysts,[7] oxidant solubilizers,[8] membrane transport agents,[9] sequestering reagents,[10] radioactive metal binders[11] and chiral chromophoric receptors,[12] to name but a few. Many of the benefits of crown ethers can be traced to their ability to encapsulate metal cations in their cyclic cavity, with a metal cation selectivity that at a simplistic level depends on the best-fit cation radius/crown ring size scenario.[13] There is a wealth of crown polycycles,[14] and numerous binding studies have been preformed using NMR spectroscopy,[15] potentiometric titrations,[16] bi-layer extraction,[17] redox response alterations[18] and luminescence quenching.[19] In particular, the simple polyethers **C4**–**C6** have been described by Bartsch,[20] Changrong,[21] Reinhoudt[22] and Bouzide,[23] although metal ion binding has been reported only by Yakshin et al.[24] This latter report concentrated on the cation-extraction properties of this class of polyether. It is noted that the compounds are related to the series of more rigid naphthalene-based crown compounds studied by Bhattacharyya.[25] Here, we describe an in-depth investigation of the cation binding properties of **C4**–**C6** (Figure 1) by fluorescence quenching, coupled with a molecular modelling study

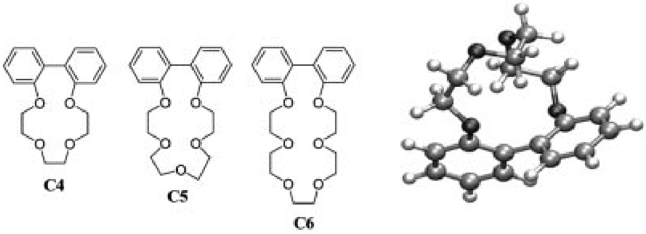

Figure 1. Structural formulae of crown ether ligands used in this study (left) and a representation of the 2,2′-biphenoxyl-based crown ether ligand **C4** (right). Ligands are named according to the number of oxygens contained in the crown ether strap.

---

[a] Molecular Photonics Laboratory, School of Natural Sciences (Chemistry), Bedson Building, University of Newcastle,
Newcastle upon Tyne, NE1 7RU, UK
Fax: + 44-191-222-8660
E-mail: a.c.benniston@ncl.ac.uk

Supporting information for this article is available on the WWW under http://www.eurjoc.org or from the author.

DOI: 10.1002/ejoc.200500550

for 1:1 cation/crown complex formation. The mechanism for fluorescence quenching by redox-inert cations is also discussed in terms of a model whereby coordination perturbs the relative energies of the emitting singlet excited states.

Results and Discussion

Synthesis

The synthetic procedure used to prepare **C5**–**C6** involved a slight adaptation of methods reported earlier;[20–23] THF was used as the solvent, and NaH was used as the base for the deprotonation of 2,2′-biphenol. Yields of the ligands were not optimised but even so were comparable with values reported previously. Because highly purified samples are needed for fluorescence spectroscopy, the polyethers were subjected to extensive column chromatography and subsequent multiple recrystallisations. Purity, and the authenticity of the crown ethers, was assessed using a range of analytical techniques. It was determined by GC–MS that during preparation of **C4** with THF as solvent and NaH as base, the dimerised (2+2) product was produced as a contaminant. This material was difficult to remove from the target crown ether. Repeated chromatographic separations failed to completely resolve the two products. The desired ligand **C4** was eventually obtained by carrying out the cyclisation reaction in DMF and using K_2CO_3 as the base. Under these conditions, the amount of dimerised side-product was significantly reduced and easily separated from the target ligand. No attempt was made to rationalise the markedly different levels of reactivity found under the two sets of conditions. It is possible that the smaller Na^+ ion functions as a better template for (2+2) adduct formation, but this possibility was not pursued.

Photophysical Studies

Absorption and fluorescence spectra were recorded for **C4**–**C6** in N_2-purged acetonitrile at room temperature. In keeping with related 2,2′-biphenyl derivatives,[26] all three crown ethers exhibit a relatively intense but featureless absorption band centred at 280 nm. There is no obvious dependence of the absorption band maximum on the length of the polyether strap, but the spectral profile is consistent with a non-planar ground state. The measured absorption coefficient of 6000 $\text{M}^{-1}\cdot\text{cm}^{-1}$ at 280 nm indicates that this band is due to the $^1A\rightarrow{}^1L_a$ transition, with the less intense $^1A\rightarrow{}^1L_b$ transition being obscured. This general behaviour is consistent with observations made earlier by Yakshin and co-workers.[24]

Relatively intense fluorescence is apparent in fluid solution and is centred around 340 nm (Figure 2); the spectral profile and peak position are insensitive to changes in excitation wavelength. The excitation spectrum matches closely with the absorption profile for each polyether while the fluorescence and absorption bands show reasonable mirror symmetry. The Stokes shifts (SS = 6215 cm^{-1}) measured for **C4**–**C6** are surprisingly large and indicate that the initial Franck–Condon state rapidly relaxes to a more favourable geometry.[27] Fluorescence quantum yields (Φ_F) are about 0.10 and only slightly dependent on the length of the polyether strap (Table 1). Fluorescence decay profiles were strictly monoexponential regardless of monitoring wavelength and unaffected by the presence of dissolved molecular oxygen. The derived fluorescence lifetimes (τ_s) are around 1.0 ns (Table 1). In general, the fluorescence yield and lifetime tend to increase with increasing strap length although the effect is modest.

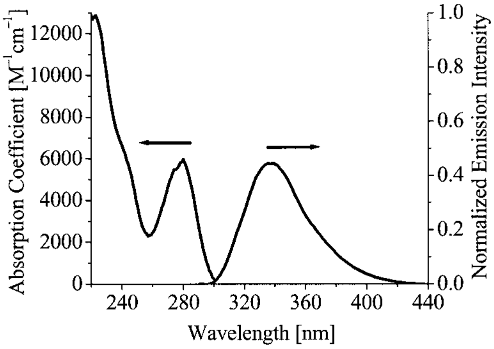

Figure 2. Absorption and emission profiles of **C5** measured in acetonitrile solution at room temperature.

Table 1. Binding constants and photophysical parameters[a] for crown ethers **C4**–**C6** measured in acetonitrile solution at room temperature.

Crown	**C4**	**C5**	**C6**
β Li^+ [M^{-1}]	3	85	68
β Na^+ [M^{-1}]	<1	465	2070
β K^+ [M^{-1}]	<1	55	7370
λ_{abs} [nm]	280	280	280
ε_{max} [$\text{mol}^{-1}\cdot\text{dm}^3\cdot\text{cm}^{-1}$]	6400	6000	6000
Stokes shift [cm^{-1}]	6215	6215	6215
λ_{fl} [nm]	340	340	340
τ_s [ns]	1.0	1.1	1.2
φ_f	0.083	0.089	0.093
k_r [s^{-1}]	8.3×10^7	8.1×10^7	7.8×10^7
k_{nr} [s^{-1}]	9.2×10^8	9.0×10^8	7.6×10^8
τ_t [μs]	16.0	16.5	18.0

[a] Parameters described in text.

For compounds **C4**–**C6**, the radiative rate constants, k_r, were calculated to be within the range $8.0\pm0.4\times10^7$ s^{-1}, thereby indicating that emission is due to the $^1A\leftarrow{}^1L_a$ transition. This is in contrast to biphenyl where $k_r = 9\times10^6$ s^{-1}, and the emission is assigned a $^1A\leftarrow{}^1L_b$ transition. It is thought that this difference in the emitting state is due to a number of factors including the alkoxy groups in **C4**–**C6** increasing the electron density on the biphenyl chromophore and a difference in the excited state conformations of the two systems. It is well known that the two lowest-lying singlet states in biphenyl are very close in energy,[28] so it is feasible that a change in geometry can affect the equilibrium between these states. For each polyether, decay of the singlet excited state is dominated by nonradiative processes.

The rate constant for nonradiative decay (k_{nr}) shows a small dependence on strap length (Table 1) and decreases as the strap becomes longer. Since the electronic factors remain fixed, this effect can be attributed to slight changes in the molecular conformation.

Laser flash photolysis studies performed with the fourth harmonic of a Nd:YAG laser (266 nm excitation) gave access to the corresponding triplet excited states of **C4**–**C6** (Supporting Information). The transient differential absorption spectra exhibit peaks at 370 nm and 410 nm, the latter being somewhat more intense. There is little variation among the compounds. Decay of the transient signal is first-order at low laser intensity but becomes biphasic at high intensities. The derived triplet lifetimes (τ_t) are around 15 µs in each case (Table 1). The shorter-lived component seen at high laser power, which is always a minor contributor and has a lifetime of ca. 2 µs, is attributed to the biphenyl π-radical cation formed by two-photon ionization. Phosphorescence can be observed in a butyronitrile matrix at 77 K, with a maximum around 450 nm and lifetimes in excess of 1 ms (Supporting Information).

Binding Studies

It has been well established that NMR is a powerful tool with which to study complexation of alkali cations with crown ethers.[15] Alterations in vicinal H,H coupling constants can be used to estimate the dihedral angle within $O(CH_2)_2O$ fragments, whereas ^{13}C chemical shifts give an insight into the degree of in-plane interactions. Initial attempts to confirm cation binding to **C4**–**C6** using ^1H- and ^{13}C NMR spectroscopic measurements suffered from severe problems. In the ^1H NMR case, shifts and coupling constant changes of the aromatic and alkoxy proton signals were too small to be measured reliably, while shifts of ^{13}C aromatic resonances were difficult to fit to a simple binding model. Electrospray mass spectrometry studies following addition of Li^+, Na^+ and K^+ cations to each of the polyethers in acetonitrile confirmed the formation of a 1:1 cation/ligand adduct. The mass spectrometry records showed no discernible peaks (>1%) attributable to stoichiometries other than 1:1. Moreover, competitive binding experiments performed for each ligand showed that the cation binding preferences were Li^+ (**C4**), Na^+ (**C5**) and K^+ (**C6**). This finding is consistent with expectations based on size.

Fluorescence spectroscopy is a useful tool for monitoring interactions between host and guest species in solution.[19] The modest fluorescence seen for compounds **C4**–**C6** led us to believe that structural modifications accompanying cation binding might be reflected in changes in yield of the spectral profile. As a generic example, Figure 3 shows an overlay of fluorescence spectra recorded during titration of **C5** with $NaClO_4$ in acetonitrile solution. Low concentrations of cation cause a marked decrease in fluorescence intensity that tends towards a plateau corresponding to about 55% quenching. Although the general shape of the fluorescence spectrum is preserved during the titration, the emission maximum shifts slightly (ca. 5 nm) towards higher energy. After the initial quenching event, further addition of salt caused a progressive decrease in fluorescence intensity without changing the spectral profile. This secondary quenching was traced to a general salt effect, since it was common to all electrolytes including large bulky ammonium cations that cannot bind to the polyether. Over this part of the titration, the fluorescence intensity decreased linearly with molar concentration of salt.

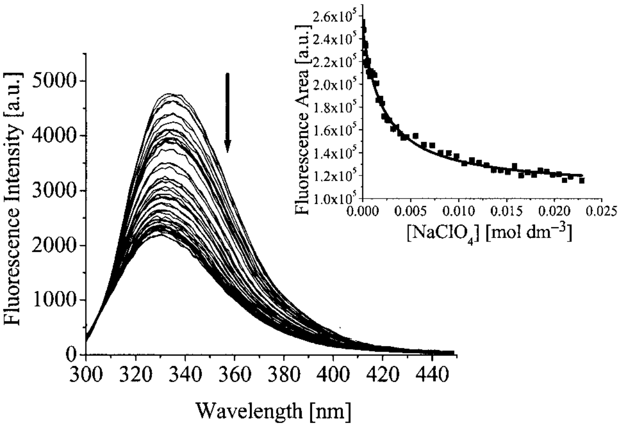

Figure 3. Fluorescence spectral changes observed for **C5** in acetonitrile upon addition of aliquots of $NaClO_4$. The inset shows the least-squares fit to the data points using a 1:1 cation-to-ligand binding model.

The initial portion of the fluorescence titration could be fitted satisfactorily to a 1:1 cation/ligand binding model. This requires only two fluorescing species; namely, the free polyether and the resultant cation complex. The binding constant β for the process (Scheme 1) was calculated from a minimum of 20 cation concentrations and was averaged over several independent runs. For the specific case of Na^+ binding to **C5**, the derived overall stability constant β has a value of $465 \pm 30\ \mathrm{M}^{-1}$. Additional thermodynamic parameters associated with cation binding were obtained by measuring β over the temperature range 278 K to 333 K. From the resultant linear van't Hoff plot (Supporting Information), the enthalpy contribution ($\Delta H°$) was found to be $+7.05\ \mathrm{kJ{\cdot}mol^{-1}}$ and the entropy factor ($\Delta S°$) was $+74.8\ \mathrm{J{\cdot}K^{-1}\ mol^{-1}}$. The large entropic contribution is attributed to desolvation of the cation and ligand, despite the obvious reduction in the degrees of freedom of the crown polycycle upon complexation. Similar experiments were used to determine β for the other cations and/or polyethers (Table 1). For binding experiments involving K^+ the hexafluorophosphate salt was used because of solubility problems with the perchlorate salt. It is assumed that no strong ion-pairing takes place, which could influence the outcome of the thermodynamic binding data.[29] In all cases, binding could be explained in terms of a 1:1 complex. On inspection of these β values it is clear that **C5** has a greater specificity for Na^+ ions, whereas K^+ prefers to bind to the larger **C6** ligand. The cation Li^+ binds very weakly to **C4** but not to the larger polyethers. The observed selectivity is fully consistent with the electrospray mass spectrometry results.

$$M + L \underset{}{\overset{\beta_1}{\rightleftharpoons}} ML \quad \beta = \frac{[ML]}{[M][L]}$$

Scheme 1.

Quenching Mechanisms

We can now address the mechanism by which the cation quenches fluorescence from the polyether. First, it is important to note that the nature of the anion has no effect on the fluorescence yield, whilst the quenching profile at low cation concentrations is highly characteristic of static quenching but is inconsistent with diffusional fluorescence quenching. These findings indicate that complexation is a necessary requirement for fluorescence quenching. None of the cations studied here are redox active and they are without low-lying electronic energy levels. As such, quenching is not due to the onset of either electron- or energy-transfer processes. Likewise, there is no correlation between the quenching efficiency and the spin-orbit coupling constants (ξ = 0.23, 11.5 and 38 cm^{-1} for Li^+, Na^+ and K^+ respectively)[30] of the cation. Complexation is not accompanied by excimer or exciplex emission, but there is a slight fluorescence spectral shift towards higher energies. This latter effect is most likely caused by the bound cation preventing the biphenyl unit from adopting the preferred excited state geometry. More specifically, the cation is expected to rigidify the polyether and thereby prevent the biphenyl chromophore from approaching a planar structure. In order to investigate this effect, we have conducted a series of molecular modelling studies.

Molecular Modelling

It is known that ground-state biphenyl in fluid solution is in dynamic motion with a torsion angle of 38° in acetonitrile.[31] Upon excitation into the lowest-energy singlet excited state the molecule becomes planar, despite the obvious steric repulsion. In compounds **C4**–**C6** the average ground-state dihedral angle in the biphenyl unit is calculated to be 130°, but molecular dynamics simulation (MDS) studies show that this angle can reach extreme values ranging from 70° to 160°. This change in geometry from the parent compound is easily rationalised in terms of the alkoxy substituents that add to the overall repulsive forces. As might be expected, the MDS studies show the polyether chain to be dynamic but expanded [Figure 4(a)]. The likelihood is that these polyethers are unable to attain a planar structure in the excited singlet state, although the observed Stokes shifts indicate substantial geometric change following excitation. The inability to become planar explains the observation that the fluorescence quantum yields and lifetimes are less than those found for biphenyl under the same conditions. The internal flexibility apparent from the MDS studies tends to obscure differences between the various polyethers, however, such that their photophysical properties remain quite comparable. That is to say, the excited singlet state will attempt to minimise the torsion angle and, since this motion will be fast, the photophysical properties are probably set by the ability to reach the minimum torsion angle.

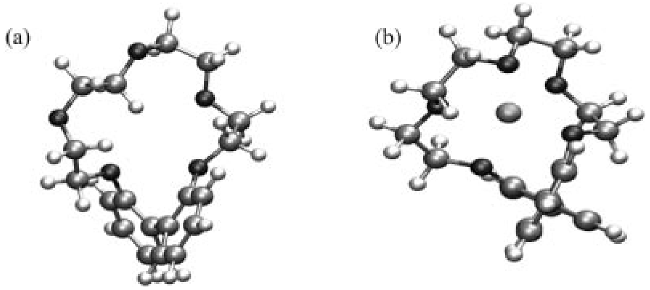

Figure 4. Molecular model of **C5** showing the expanded polyether strap (a) and the resultant structure upon cation binding to three of the five possible oxygen atoms (b).

The MDS studies indicate that the cation binds to the polyether so as to give a variety of similar structures that differ only slightly in energy. Indeed, for each reactant pair, a family of stable structures can be observed. Taking **C5** as a typical case, we find that at any given moment the cation binds to the three oxygen atoms. The preference lies with oxygen atoms in the polyether chain, but the phenoxyl oxygen atoms are also used in binding the cation [Figure 4(b)]. Coordination of a cation at the polyether void causes several notable effects; the structure becomes less dynamic, the central torsion angle changes and the range of accessible angles becomes dampened. Overall there is a rigidification of the structure. However, the structure is still dynamic, and the torsion angle fluctuates about a mean value (Figure 5). The effect of Li^+ and Na^+, in particular, is quite noticeable, and the average angle changes from 130° (50°) for the parent to 55° for Li^+ and 65° for Na^+. There is also a considerable alteration in the torsion angle range when we move from **C5** (70–165°) to Li^+ (23–99°) and Na^+ (30–105°). The larger K^+ ion does not fit well inside the cavity, and there is more variation in the average torsion angle, the mean value being around 91°. A similar trend is seen for **C6**, where the mean angle changes from 120° for the parent

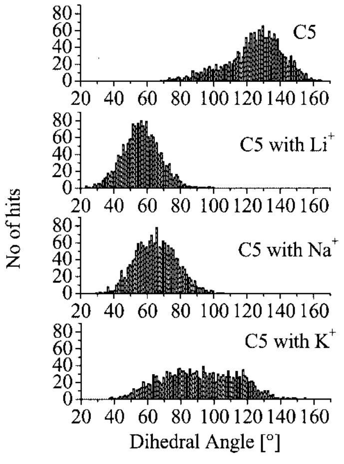

Figure 5. Histograms showing the variation in the dihedral angle upon cation binding.

to 65° and 70° for the corresponding Na^+ and K^+ complexes, respectively.

Overall, it appears that the fluorescence quantum yields and lifetimes for these polyethers are dependent on the torsion angle around the biphenyl group. Planar geometries favour higher yields and longer lifetimes. This effect might be due to different levels of mixing between the ^1L_a and the ^1L_b states or to changes in the degree of electron delocalisation. Whatever the exact reason for the effect, it provides a simple means by which to monitor the torsion angle in solution.

The titration data show that the fluorescence quantum yield continues to decrease with increasing salt concentration after complexation is complete. Under such conditions, the change in fluorescence correlates with the ionic strength. This effect can be explained in terms of osmotic pressure where the solute molecule exerts pressure on the polyether chain. Increasing the solute concentration causes the polyether to shrink and to become more rigid. This has the effect of restricting the range of available torsion angles. If we accept that the photophysical properties are set by the minimum torsion angle, additional salt will lower the fluorescence yield. Consistent with this hypothesis is the realisation that, whereas the primary quenching event is highly sensitive to the type of cation, secondary quenching is independent of the nature of the salt.

Conclusions

We have synthesised a series of crown ether ligands based upon the 2,2′-biphenyl unit. In the series, the length of the polyether chain increases progressively. Binding of a single cation at the cavity defined by the crown is apparent by both mass spectrometry and fluorescence spectroscopy. The binding constants calculated from the fluorescence spectral titrations are modest, presumably because the linear biphenyl unit restricts the ability of the polyether to wrap around the cation. Complexation affects the fluorescence properties by controlling the average conformation around the emitting biphenyl group. The optimum conformation for the excited singlet state has the two phenylene rings held in a coplanar arrangement, but this geometry is inaccessible for the polyethers. The bound cation imposes additional restrictions on the geometry and forces the rings further from planarity. According to the molecular mechanics computations, this variation in angle can be quite significant (Figure 5). Thus, despite the restricted binding constants, the choice of cation allows predetermined selection of the average torsion angle. Values range from 55° to 75° and are markedly different from the corresponding torsion angles determined for the parent polyether.

The problem now is to devise a satisfactory means for exploiting this effect. On the basis of earlier work[1] relating to hole transfer across biphenyl spacers, we might anticipate something like an 80-fold variation in rate constant when the torsion angle changes from 0° to 90°. This is a sufficiently large disparity to provide for selectivity in the direction of electron transfer in the event of a system being equipped with a dual pathway where individual routes differ in terms of torsion angle. Switching the conformation by rapid injection of a cation would, in the most extreme case, give an angle change of ca. 60°. There is a modest degree of specificity for particular cations that could be used to fine-tune the system. Thus, these materials hold promise for use as bridges in molecular photonic devices aimed at directing charge along one of several pathways. An obvious limitation is the slow switching times since these are based on physical injection and removal of cation.

A second interesting feature of these systems relates to the observation that the molecular conformation can be perturbed by osmotic pressure. Here, the nature of the solute is unimportant, but the pressure exerted on the polyether translates to a variation in the central biphenyl torsion angle. This is a linear effect whereby contraction of the polyether increases progressively with increasing solute concentration. As such, the effect could be exploited to develop artificial muscles that operate without the need for electrical stimulation. Building the biphenyl bridge into a liquid crystal might provide a means for systematic variation of birefringence by careful variation of pressure. Such studies are on-going in our laboratory.

Experimental Section

All raw materials were purchased from commercial sources and used as received. Solvents were dried by standard literature methods[32] before being distilled and stored under nitrogen over 4 Å molecular sieves. ^1H and ^{13}C NMR spectra were recorded with a JEOL Lambda 500 MHz or Bruker AVANCE 300 MHz spectrometers. Routine mass spectra and elemental analyses were obtained using in-house facilities.

General Procedure for the Synthesis of C5 and C6: A solution of 2,2′-biphenol (1 equiv.), sodium hydride (2 equiv.) and THF (20 mL) was stirred for 2 h at 40 °C. Using a syringe pump, a solution of tetra-(penta-)ethylene glycol ditosylate (1 equiv.) in THF (50 mL) was added over the course of 13 h. After addition, the reaction mixture was refluxed for 16 h. The solvent was removed under reduced pressure and the white residue dissolved with a mixture of DCM/water. The separated organic layer was washed with NaOH (aq) until neutral and then with H_2O. The organic layers were combined, dried with magnesium sulfate, and the solvents were evaporated. The resultant yellow oil was purified by flash column chromatography on silica gel and elution with ethyl acetate/petroleum ether (2:1). The residue remaining after removal of the appropriate fractions was washed with methanol and dried to yield the desired product.

C5: 2,2′-Biphenol (1.49 g, 7.98 mmol), tetraethylene glycol ditosylate (3.5 g, 7.98 mmol), sodium hydride (60%, mineral oil), (0.64 g, 15.9 mmol). Product afforded as white crystals, yield (300 mg, 0.87 mmol, 12%), m.p. 90–92 °C. ^1H NMR (300 MHz. $CDCl_3$): $\delta = 7.23$ (m, 2 H, ArH), 7.15 (dd, 2 H, $J = 7.4$ Hz, 1.8 Hz, ArH), 6.95 (m, 4 H, ArH), 4.20 (m, 2 H, CH_2), 3.95 (m, 2 H, CH_2), 4.65 (m, 12 H, CH_2) ppm. ^{13}C NMR (300 MHz. $CDCl_3$): $\delta = 156.93$ (ArC-O), 131.68 (ArC), 129.0 (ArC-ArC), 128.85 (ArC), 120.85 (ArC), 112.37 (ArC), 71.48 (CH_2), 71.37 (CH_2), 70.08 (CH_2), 68.21 (CH_2) ppm. MS (EI): $m/z = 344.1617$ (M^+ requires 344.1624). $C_{20}H_{24}O_5$ (344.4): calcd. C 69.75, H 7.02; found C 69.67, H 7.11.

C6: 2,2′-Biphenol (0.88 g, 4.76 mmol), pentaethylene glycol ditosylate (2.6 g, 4.76 mmol), sodium hydride (60 %, mineral oil), (0.38 g, 9.51 mmol). Product afforded as white crystals, yield (330 mg, 0.85 mmol, 20 %), m.p. 44–46 °C. ^{1}H NMR (300 MHz. $CDCl_3$): δ = 7.22 (m, 2 H, ArH), 7.15 (dd, 2 H, J = 7.4 Hz, 1.7 Hz, ArH),6.90 (m, 4 H, ArH), 4.02 (m, 4 H, CH_2), 3.55 (m, 16 H, CH_2) ppm. ^{13}C NMR (300 MHz. $CDCl_3$): δ = 156.91 (ArC-O), 131.66 (ArC), 129.07 (ArC-ArC), 128.83 (ArC), 120.97 (ArC), 112.65 (ArC), 71.26 (CH_2), 71.13 (CH_2), 70.10 (CH_2), 68.43 (CH_2) ppm. MS (EI): m/z = 388.1901 (M^+ requires 388.1886). $C_{22}H_{28}O_6$ (388.5): calcd. C 68.02, H 7.27; found C 67.85, H 7.34.

Procedure for the Synthesis of C4: 2,2′-Biphenol (0.5 g, 2.685 mmol) and potassium carbonate (1 g, 7.2 mmol) was suspended in dry DMF (100 mL) and heated at 85 °C for 1.5 h. Triethylene glycol ditosylate (1.58 g, 3.22 mmol) dissolved in DMF (20 mL) was added over the course of 14 h using a syringe pump. After addition, the mixture was left to reflux overnight. The solvent was removed under reduced pressure and the yellow residue extracted into chloroform, which was washed with water until neutral. The organic fractions were dried with magnesium sulfate, and the solvents were evaporated. The product was purified by flash column chromatography on silica gel, eluting first with ethyl acetate/petroleum ether (1:1) and then with ethyl acetate/petroleum ether (4:1). The oil obtained after removal of the appropriate fractions was washed with methanol and dried to give the desired product as a white powder. Yield (280 mg, 0.93 mmol, 37 %), m.p. 102–104 °C. ^{1}H NMR (300 MHz. $CDCl_3$): δ = 7.22 (m, 2 H, ArH), 7.10 (dd, 2 H, J = 7.4 Hz, 1.8 Hz, ArH), 6.87 (m, 4 H, ArH), 4.20 (m, 2 H, CH_2), 3.87 (m, 2 H, CH_2), 3.71 (m, 4 H, CH_2), 3.51 (m, 4 H, CH_2) ppm. ^{13}C NMR (500 MHz. $CDCl_3$): δ = 156.43 (ArC-O), 131.26 (ArC), 128.74 (ArC-ArC), 128.36 (ArC), 120.16 (ArC), 111.16 (ArC), 70.41 (CH_2), 69.83 (CH_2), 67.11 (CH_2) ppm. MS (EI): m/z = 300.1368 (M^+ requires 300.1362). $C_{18}H_{20}O_4$ (300.4): calcd. C 71.98, H 6.71; found C 71.48, H 6.69.

Photophysical Measurements: Absorption spectra were recorded with a Hitachi U3310 spectrophotometer while corrected luminescence spectra were recorded with a Hitachi F4500 spectrophotometer. All luminescence measurements were made using optically dilute solutions and were corrected for spectral imperfections of the instrument by reference to a standard lamp. Emission quantum yields were measured relative to biphenyl (φ_f = 0.18).[28] Fluorescence lifetimes were measured with a Spex Fluorolog tau-3 spectrophotometer. Laser flash photolysis studies were carried out with an Applied Photophysics LKS60 spectrometer. Excitation was provided with a frequency-quadrupled, Q-switched Nd:YAG laser (266 nm, FWHM = 4 ns). Transient differential absorption spectra were recorded point-by-point, while decay kinetics were measured at various detection wavelengths and signal averaged. Solutions were thoroughly purged with N_2 before each experiment.

General Experimental Procedure for Fluorescence Titrations: Spectrophotometric titrations were performed by adding small aliquots of a standard solution of $MClO_4$ (M = Li^+, Na^+) and KPF_6 (0.1 м) (this salt was used because of solubility problems with the perchlorate salt) in acetonitrile to a dilute solution of **C4**–**C6** (1×10^{-5} м) in spectroscopic-grade acetonitrile. Analysis of the fluorescence spectral titration data was made as follows: Firstly, a complete spectral analysis was made using SPECFIT with the known spectra for the free ligand and for the 1:1 complex. This analysis allowed determination of the relative fluorescence yields for the free ligand and the 1:1 complex. The analysis indicated that only two fluorescing species were involved. Secondly, a quantitative analysis was made by fitting the fluorescence intensity at a single wavelength, measured at different cation concentrations, to a set of model equations. Stability constants were derived by fitting experimental data collected at 10 different wavelengths and for at least 20 different cation concentrations. The results from three separate titrations were averaged to give the quoted binding constant. All data were corrected for minor dilution effects.

Molecular Modelling: Computational studies were performed with several different packages. Minimum energy conformations were obtained using the Gaussian03 and Insight II programs. Several geometry optimisations were performed, starting from different initial geometries, using the semi-empirical PM3 method and the HF method with a 6-311G basis set. All calculations were run in vacuo and in the absence of the counterions. Good agreement was found between the various methods used. For calculations performed with Insight II, potentials were assigned using a modified ESFF force-field and geometry optimisations were performed using the Newton method. Convergence was achieved when a gradient of 0.00001 was reached. Minimised structures were used as a starting point for the molecular dynamics simulations (MDS). These MDS studies were set up in two stages with 10 ps of equilibration time and 20 ps of run time, the temperature being set at 295 ± 5 K. A comprehensive set of data was saved every 10 fs of simulation.

Supporting Information (see footnote on the first page of this article) contains the van′t Hoff plot, the triplet-triplet absorption and phosphorescence spectra of **C4** and histograms showing the variation in the dihedral angle upon cation binding to **C6**.

Acknowledgments

This work was supported by the EPSRC (GR/R2305/01) and the University of Newcastle.

---

[1] A. C. Benniston, A. Harriman, P. Li, C. A. Sams, M. D. Ward, *J. Am. Chem. Soc.* **2004**, *126*, 13630–13631.
[2] M. M. Toutounji, M. A. Ratner, *J. Phys. Chem. A* **2000**, *104*, 8566.
[3] A. Helms, D. Heiler, G. McLendon, *J. Am. Chem. Soc.* **1991**, *113*, 4325–4327.
[4] A. C. Benniston, P. Li, C. A. Sams, *Tetrahedron Lett.* **2003**, *44*, 3947–3949.
[5] W. Wallace, C. Chen, E. M. Eyring, S. Petrucci, *J. Phys. Chem.* **1985**, *89*, 1357–1366.
[6] C. J. Pedersen, *J. Am. Chem. Soc.* **1967**, *89*, 7017–7036.
[7] M. Hager, K. Holmberg, *Chem. Eur. J.* **2004**, *10*, 5460–5466.
[8] D. J. Sam, H. E. Simmons, *J. Am. Chem. Soc.* **1972**, *94*, 4024–4025.
[9] P. K. Mohapatra, D. S. Laksmi, D. Mohan, V. K. Manchanda, *J. Membr. Sci.* **2004**, *232*, 133–139.
[10] a) G. Downie, J.-G. Mao, H. Parmar, A. M. Guloy, *Inorg. Chem.* **2004**, *43*, 1992–1997; b) J. C. Aguilar, E. R. de San Miguel, J. de Gyves, R. A. Bartsch, M. Kim, *Talanta* **2001**, *54*, 1195–1204.
[11] H. Stephan, H. Spies, B. Johannsen, K. Gloe, M. Gorka, F. Vögtle, *Eur. J. Inorg. Chem.* **2001**, 2957–2963.
[12] E. P. Kyba, G. W. Gokel, F. De Jong, K. Koga, L. R. Sousa, M. G. Siegel, L. Kaplan, G. Dotsevi, Y. Sogah, D. J. Cram, *J. Org. Chem.* **1977**, *42*, 4173–4184.
[13] J. W. Steed, *Coord. Chem. Rev.* **2001**, *215*, 171–221.
[14] R. M. Izatt, K. Pawlak, J. S. Bradshaw, R. L. Bruening, *Chem. Rev.* **1991**, *91*, 1721–2085.
[15] A. Wong, G. Wu, *J. Phys. Chem. A.* **2000**, *104*, 11844–11852.
[16] H. J. Buschmann, E. Schollmeyer, *J. Electroanal. Chem.* **1999**, *474*, 188–191.
[17] A. M. Costero, J. Sanchis, S. Peransi, S. Gil, V. Sanz, A. Domenech, *Tetrahedron* **2004**, *60*, 4683–4691.

[18] A. C. Hall, C. Suarez, A. Choudhury-Hom, A. N. A. Manu, C. D. Hall, G. J. Kirkovits, I. Ghiriviga, *Org. Biomol. Chem.* **2003**, *1*, 2973–2982.
[19] a) J. Cody, C. J. Fahrni, *Tetrahedron* **2004**, *60*, 11099–11107; b) L. J. Charbonniere, R. Ziessel, C. A. Sams, A. Harriman, *Inorg. Chem.* **2003**, *42*, 3466–3474.
[20] B. Czech, A. Czech, R. A. Bartsch, *J. Heterocycl. Chem.* **1984**, *21*, 341–343.
[21] C. Niu, X. Liu, C. Wu, *Huaxue Shiji* **1985**, *7*, 15–16.
[22] D. N. Reinhoudt, D. de Jong, E. M. Van de Vondervoort, *Tetrahedron* **1981**, *37*, 1753–1762.
[23] A. Bouzide, G. Sauvé, *Org. Lett.* **2002**, *4*, 2329–2332.
[24] V. V. Yakshin, O. M. Vilkova, S. A. Kotlyar, R. Ya. Grigorash, *Dok. Acad. Nauk* **2001**, *379*, 80–82.
[25] S. Bhattacharyya, L. R. Sousa, S. Ghosh, *Chem. Phys. Lett.* **1997**, *269*, 314–320.
[26] a) M. T. Shaughnessy, W. H. Rodebush, *J. Am. Chem. Soc.* **1941**, *63*, 3018–3025; b) I. B. Berlman, *J. Chem. Phys.* **1970**, *52*, 5616–5621.
[27] H.-S. Im, E. R. Bernstein, *J. Chem. Phys.* **1988**, *88*, 7337–7347.
[28] I. B. Berlman, *J. Phys. Chem.* **1970**, *74*, 3085–3093.
[29] Y. Liu, H.-Y. X.-P. Bai, T. Wada, Y. Inoue, *J. Org. Chem.* **2000**, *65*, 7105–7109.
[30] S. L. Murov, *Handbook of Photochemistry*, Dekker, New York, **1973**.
[31] M. Akiyama, T. Watanabe, M. Kakihana, *J. Phys. Chem.* **1986**, *90*, 1752–1755.
[32] D. D. Perrin, W. L. F. Armarego, *Purification of Laboratory Chemicals, 3rd Edition*, Permagon Press Ltd, Oxford, **1988**.

Received: July 21, 2005